

Study on Shield Operation Method in Soft Ground by Shield Simulation

Mitsutaka Sugimoto¹, Hideyuki Tanaka², Ngoc Thi Huynh³, Salisa Chaiyaput⁴, Le Gia Lam⁵ and Jian Chen⁶

¹Professor, Nagaoka University of Technology, Nagaoka, Japan

²Graduate School of Nagaoka University of Technology, Nagaoka, Japan

³Lecturer, Vietnam National University Hochiminh City, University of Technology, Vietnam

⁴Lecturer, Faculty of Engineering, King Mongkut's Institute of Technology Ladkrabang, Thailand

⁵Lecturer, Can Tho University, Can Tho, Vietnam

⁶Associate Professor, Harbin Institute of Technology, Harbin, China

E-mail: sugimo@vos.nagaokaut.ac.jp

ABSTRACT: Shield tunneling technologies have been developed for constructing tunnels in soft ground especially under groundwater. Recently, challenging projects from the viewpoint of tunneling technology have been planned. To realize these constructions, it is necessary to examine the shield operation method preliminarily. The authors have developed a method to carry out the above examination and have confirmed its validity for a tunnel in stiff ground. In this research, to examine the performance of the proposed method for soft ground tunnel, the simulation on shield behavior was carried out using the estimated shield operational data for a tunnel in soft ground. As a result, the following were found: the shield steering conditions by the proposed method are not enough to rotate the shield along a sharp curve in case of soft soil; and the simulation results have a good agreement with the planned alignment using proper shield operational data.

KEYWORDS: Shield tunneling method, Kinematic shield model, Articulated shield, Steering, Numerical simulation

1. INTRODUCTION

Shield tunneling technologies have been developed for constructing tunnels in soft ground especially under groundwater. In particular, the closed-type shield has been developed together with computer-aided automatic control systems. However, these systems are based on empirical relationships and do not have a precise theoretical background. Therefore, it is sometimes difficult to control the shield in a complicated geological formation and to predict the shield behavior without case records. To solve such problems, it is necessary to simulate the shield behavior such as the deviation and the rotation of the shield during excavation theoretically, taking into account the balance of the loads acting on the shield. Furthermore, recently, challenging projects from the viewpoint of soft ground tunneling technology have been planned, such as a spiral twin tunnel constructed by the horizontal and vertical variation shield method (H&V shield), as shown in Figure 1 (Muto et al. 2015), and a tunnel with a sharp curve in three-dimensional space (Miki et al. 2016). To realize these projects, the simulation of shield behavior is necessary to examine the shield operation method preliminarily and to estimate the external force acting on the shield for shield design. If there are no case records, the initial shield operation data are required for the simulation of shield behavior.

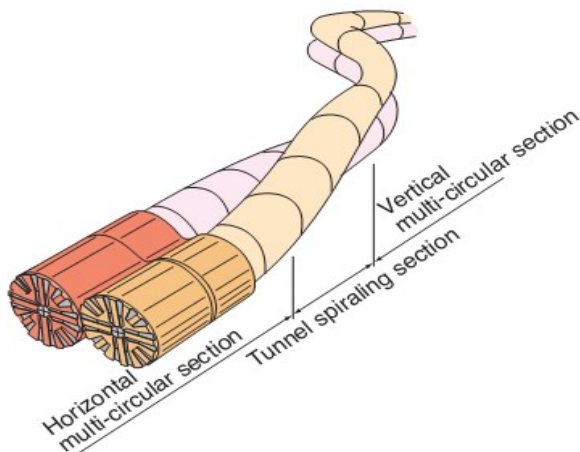


Figure 1 H&V shield (Spiral mode). (STA 2011a)

Shield behavior has been studied by both statistical and theoretical methods. The former method is used to predict and control the shield behavior by statistically obtaining a certain relationship between shield behavior and shield operational data (Szecky 1966; Sakai and Hoshitani 1987; Kuwahara et al. 1988; Shimizu and Suzuki 1992a; Shimizu et al. 1992b). From the viewpoint of engineering practices, these methods are useful, since the shield can be controlled by using up-to-date unknown parameters in the formulation based on measured data during excavation. However, these methods cannot control the shield at a sharp curve and predict the shield behavior without case records.

The latter method is used to predict and control the shield behavior based on the equilibrium conditions of force and moment acting on the shield. To clarify the shield behavior and the behavior of the surrounding ground, numerical methods, such as Finite element method (FEM) and Discrete element method, have been adopted (e.g., Finno and Clough 1985; Akagi and Komiya 1993; Komiya et al. 1999; Kasper and Meschke 2004; Melis and Medina 2005; Alsahly et al. 2013). These methods cannot represent the overcut effect, which is considered to be the predominant factor affecting the shield behavior from the viewpoint of practice (e.g., Clough et al. 1983; Rowe et al. 1983; Hansmire and Cording 1985; Fujita 1989; Lee et al. 1999; Festa 2013). Furthermore, numerical methods taking into account the gap between excavated surface and tunnel lining have been proposed (Lee et al. 1992; Rowe and Lee 1992; Takeda et al. 1998; Date et al. 1999). However, these numerical methods cannot simulate the immediate ground movement during excavation, since the shield movement is required as known conditions in these numerical methods and it depends on the past shield movement and the past excavated area.

The authors have proposed the kinematic shield model, taking into account shield tunnel engineering practices, namely, the excavated area, the tail clearance, the rotation direction of the cutter disc, sliding of the shield, ground loosening at the shield crown, and the dynamic equilibrium condition (Sugimoto 1995; Sugimoto and Sramoon, 2002a). This model is a function of shield operations, shield behavior and ground properties. Here, shield operations mean the operational control of the shield during excavation, such as jack thrust, jack moments, and applied pressure in the chamber; shield behavior means the shield position and shield rotation during excavation; and ground properties mean coefficients of earth pressures, coefficients of ground reaction, and frictional parameters, among others. The model was validated by the shield behavior

simulation of a single body shield (Sramoon et al. 2002; Sugimoto et al. 2007), those of an articulated shield (Sugimoto et al. 2002b; Sugimoto et al. 2007; Matsumoto et al. 2009), those of an H&V shield (Chaiyaput et al. 2015; Huynh et al. 2017), and those of a developing parallel link excavating shield method (DPLEX shield) (Sugimoto et al. 2003). Here, H&V shield, which is manufactured by connecting two articulated shields at their rear bodies, can construct a spiral twin tunnel, as shown in Figure 1, and DPLEX shield, of which cutter frames are driven by parallel link crank shafts on rotary shafts, can decrease cutter torque drastically due to the small radius of rotation, as shown in Figure 2.

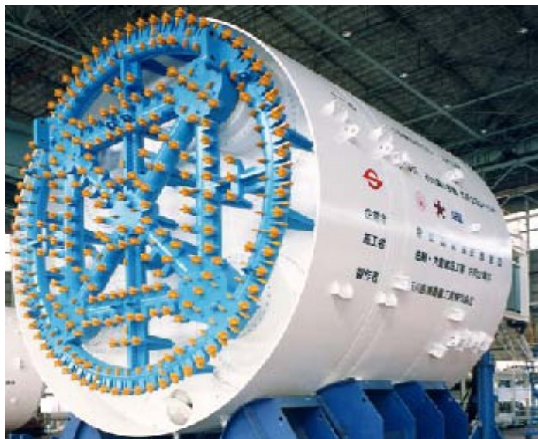


Figure 2 DPLEX shield. (STA 2011b)

On the other hand, shield direction is controlled by jack, copy cutter, and articulation mechanism in practice. The jack generates thrust and horizontal and vertical moments, which can be determined by jack pattern and shield jack pressure. The copy cutter can carry out overcut with a specified depth and a specified range along the circumference of the cutter face. The overcut by the copy cutter can reduce the ground reaction force at the overcutting range, which makes the shield rotate toward the overcut range easily. The articulation mechanism of articulated shield can crease shield with a specified direction and a specified angle. The crease of shield can reduce ground reaction force at curves by fitting the shield for its excavation area, which makes the shield rotate easily. But since these three functions have a high colinearity to shield behavior, it is difficult to obtain a unique solution at once. To solve this problem, the authors have developed the following method (Huynh 2015):

1. The copy cutter length and range and the articulation angle and direction are determined uniquely, based on geometric conditions under some constraint conditions (Chen 2008). This method can deal with horizontal and vertical curved alignments at the same position, which is called 3D compound alignment.
2. After determining the steering parameters on the copy cutter and the articulation of the shield, the initial jack force is calculated by a sequential analysis using the kinematic shield model.
3. Those values are modified so that the calculated shield behavior has a good agreement with the planned one.

In case of stiff ground, when the steering condition calculated by the above method is used for the simulation of shield behavior, the calculated shield behavior has a good agreement with the planned tunnel alignment (Miki et al. 2016; Huynh 2015). In this research, to examine the applicability of the proposed method for soft ground, the analysis conditions in soft ground were assumed, and the simulation on shield behavior was carried out using the determined shield operational parameters. This paper briefly introduces the calculation method on shield steering parameters and the kinematic shield model, shows the calculated results, and finally discusses the applicability of the proposed model quantitatively for soft ground,

comparing the calculated shield behavior with the planned tunnel alignment.

2. METHODOLOGY

In this section, the method for articulated shield is described.

2.1 Shield steering

This section shows the method to determine copy cutter length and range, and articulation angle and direction uniquely, based on geometric conditions under some constraint conditions (Chen 2008).

2.1.1 Classification of calculation conditions

From the viewpoint of geometric conditions, shield is classified into three types according to the maximum length among L_1 , L_{CSE} , and L_2 in Figure 3, as shown in Table 1:

- L_1 : $L_{M1} - L_{CSE}$
- L_2 : $L_{M2} - L_{CSE}$
- L_{M1} : length of front body
- L_{M2} : length of rear body
- L_{CSE} : length from crease center to segment front end

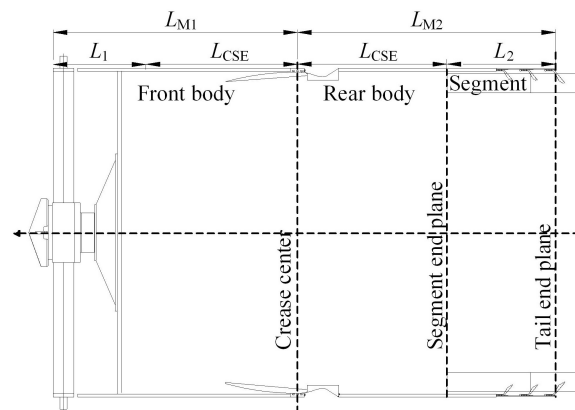


Figure 3 Dimension of articulated shield

Table 1 Machine types

Machine type	$\max(L_1, L_{CSE}, L_2)$
1	L_1
2	L_{CSE}
3	L_2

On the other hand, from the viewpoint of tunnel alignment, tunnel position is classified into four sections, as shown in Figure 4:

1. straight section
2. around the beginning of the curve (BC) section
3. curve section
4. around the end of the curve (EC) section

Figure 4 shows the geometric conditions at each section for each machine type. On different excavation sections, different operation rules should be considered.

2.1.2 Calculation conditions

The following conditions were assumed in the method:

1. The center of the segment end, P_{CSE} , follows the planned tunnel alignment.
2. The axis direction of the rear body is the tangential direction of the planned tunnel alignment at P_{CSE} .
3. The articulation angle is determined so that the copy cutter length at the concave side of the curve is minimized for type 1,

and the articulation angle is determined so that the copy cutter length at the convex side of the curve is minimized for types 2 and 3.

- The copy cutter length and range are determined so that the shield body does not push the ground, that is, the shield exists inside the excavated space.

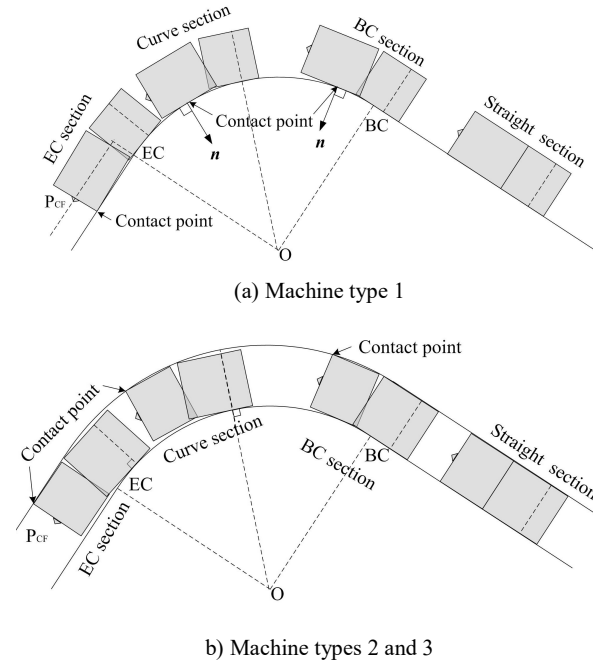


Figure 4 Trace of shield

2.1.3 Calculation procedure

Figure 5 shows the flowchart to determine the articulation condition and the copy cutter condition on a 3D compound alignment. The calculation procedure is as follows:

- The shield axis direction of the rear body and the coordinates at P_{Cr} are calculated using the planned tunnel alignment under conditions 1 and 2.
- The articulation angle and direction are calculated using a geometric condition under condition 3.
- The shield axis direction of the front body is calculated using the above results.
- The copy cutter length and range are determined by the length from the circumference of the cutter face to the most outer trace of the front body and rear body under condition 4.

2.2 Shield behavior simulation

2.2.1 Kinematic shield model

The kinematic shield model is composed of five forces: force due to self-weight of machine f_1 , force on the shield tail f_2 , force due to jack thrust f_3 , force on the cutter disc f_4 , and force on the shield periphery f_5 , as shown in Figure 6 (Chen et al. 2008). In case of the articulated shield, f_1 and f_5 act on both sections of the shield, f_3 comes from shield jacks and articulation jacks, and f_2 and f_4 act on the rear section and the front section, respectively.

The force on the shield periphery f_5 is due to the earth pressure acting on the shield skin plate and the dynamic friction force on the shield skin plate. Since the earth pressure is relied on the ground deformation, to estimate the earth pressure on shield periphery, the following were assumed:

- The shield is regarded as a rigid body.

- The ground reaction curve, which shows the relationship of the distance from the original excavated surface normal to the shield skin plate, U_n , and the coefficient of earth pressure, K , in vertical and horizontal directions, can be represented by the following functions, as shown in Figure 7 (Sramoon and Sugimoto 1999).

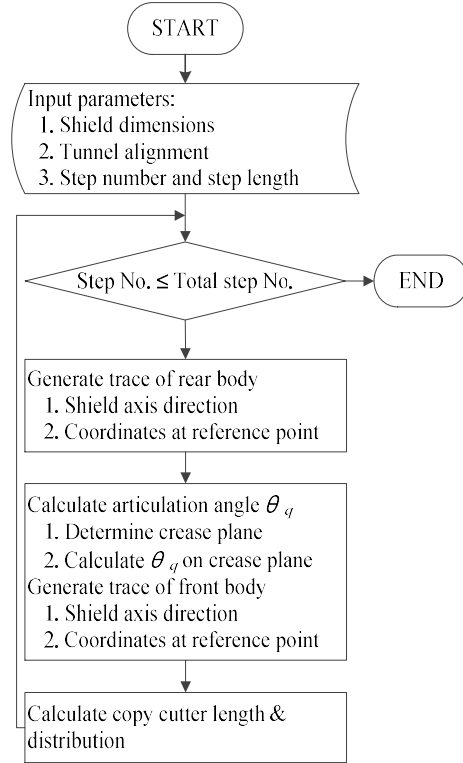


Figure 5 Flowchart of numerical procedure

$$K_i(U_n) = \begin{cases} (K_o - K_{i,min}) \tanh \left[\frac{aU_n}{K_o - K_{i,min}} \right] + K_o & (U_n \leq 0) \\ (K_o - K_{i,max}) \tanh \left[\frac{aU_n}{K_o - K_{i,max}} \right] + K_o & (U_n \geq 0) \end{cases} \quad (i = v \text{ or } h) \quad (1)$$

where a = the gradient of the functions $K(U_n)$ at $U_n = 0$, which is defined as the coefficient of subgrade reaction k divided by the overburden earth pressure σ_{vo} ; the subscripts v , h = the vertical and the horizontal directions, respectively; and the subscripts o , min , max = the initial, lower limit, and upper limit of the coefficient of earth pressure, respectively. Here it is noted that K at $U_n = 0$ is the coefficient of earth pressure at rest, K_o .

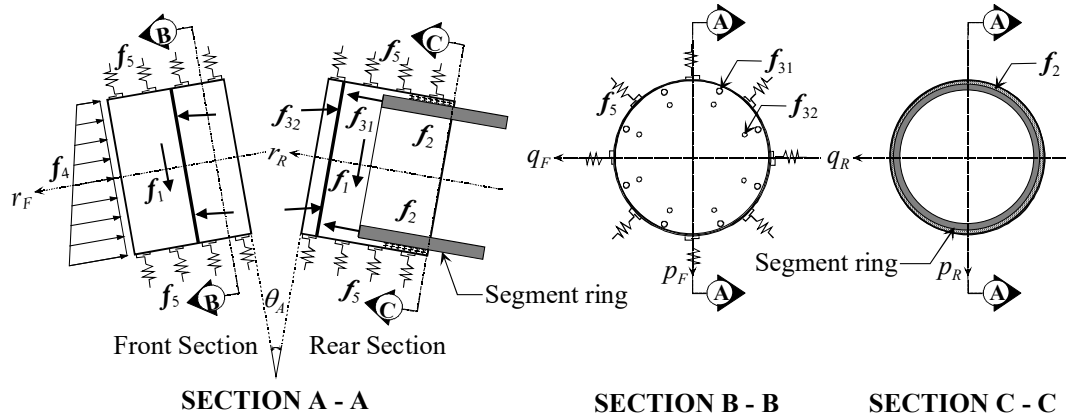
- The coefficient of earth pressure in the normal direction at any position, K_n , can be interpolated by using K_v and K_h as

$$K_n(U_n, \theta) = K_v(U_n) \cos^2 \theta + K_h(U_n) \sin^2 \theta \quad (2)$$

where θ = the angle measured from the bottom to the point in the transverse cross section.

- The earth pressure normal to the shield periphery, σ_n , can be estimated from

$$\sigma_n = K_n(U_n, \theta) \sigma_{vo} \quad (3)$$



f_1 : self-weight of machine f_2 : force on shield tail f_{31} : force due to shield jack thrust
 f_{32} : force due to articulate jack thrust f_4 : force acting at face f_5 : force acting on shield periphery
 θ_A : articulated angle

Figure 6 Model of loads acting on articulated shield

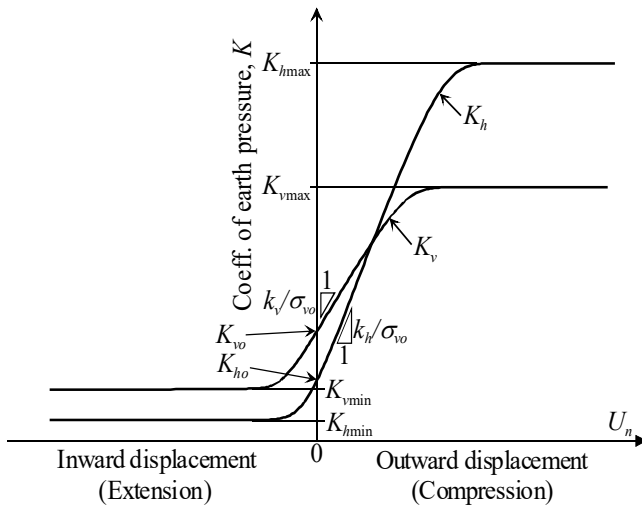


Figure 7 Ground reaction curve

The displacement of the excavated surface normal to the shield skin plate, d_n , is defined as follows, as shown in Figure 8:

1. When the shield skin plate is outside of the original excavated surface, the earth pressure is in the compression state, since the shield pushes the ground. Therefore, d_n is equal to U_n .
2. When the shield skin plate is inside of the original excavated surface and outside of the excavated surface after deformation, the earth pressure is in the extension state. Since the excavated surface after deformation contacts the shield skin plate, d_n is the same as U_n .
3. When the shield skin plate is inside of the excavated surface after deformation, the original excavated surface moves freely until its deformation stops and there is a gap between the excavated surface and the shield skin plate. In this case, there is no earth pressure acting on the shield skin plate. Thus, d_n is defined as the distance from the original excavated surface to the excavated

surface after deformation. In this case, d_n is defined as U_n when K_n reaches minimum, as shown in Figure 7. This phenomenon is due to the self-stabilization of the ground especially in the case of stiff ground.

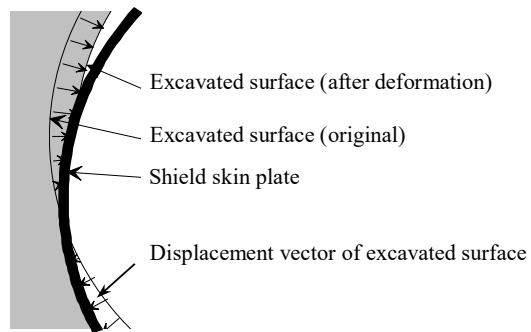


Figure 8 Displacement of excavated surface

It should be noted that the position of the original excavated surface and the shield skin plate can be determined by the observed shield position and rotation or by the simulated ones based on the shield tunneling operation. Therefore, U_n can be calculated geometrically by taking account of the shield tunneling excavation condition and the position and rotation of the shield. Considering the displacement of the excavated surface is similar to a contact problem in FEM.

2.2.2 Simulation algorithms

Here, the following coordinate systems were used to model each force, as illustrated in Figure 9. The global coordinate system C^T is selected so that the x-axis is vertically downward and the y and z-axes are on a horizontal plane. The machine coordinate system C^M is selected so that the p-axis is vertically downward without the

rotation of shield and the r-axis is in the direction of the machine axis. Here, the origin of C^M was selected at the center of the articulation on the shield axis.

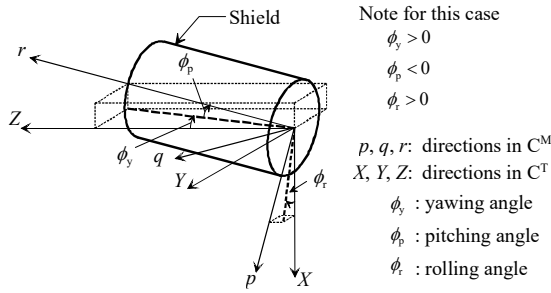


Figure 9 Definitions of a coordinate system

The shield behavior is represented by the shield movement and the shield postures (yawing angle ϕ_y , pitching angle ϕ_p , and rolling angle ϕ_r), as illustrated in Figure 9. Since the change of ϕ_r is limited in practice, the factor of shearing resistance due to the cutter torque α_{SG} was adopted as the parameter instead of ϕ_r . The shield behavior during excavation can be obtained by solving the following equilibrium conditions:

$$\begin{bmatrix} \sum_{i=1}^5 (F_{Fi}^M + F_{Ri}^M) \\ \sum_{i=1}^5 (M_{Fi}^M + M_{Ri}^M) \end{bmatrix} = 0 \quad (4)$$

where F and M are the force and moment vectors, respectively; the subscripts F and R denote the front and rear sections of the shield, respectively; the superscript M shows the machine coordinate system; and the subscripts 1 to 5 represent the component of force f_i to f_5 , respectively.

2.2.3 Index of shield behavior

Since a shield performs in three-dimensional space, the shield behavior has six degrees of freedom, so the traces of shield in horizontal and vertical planes, ϕ_y , and ϕ_p represent the shield behavior adequately.

3. APPLICATION

3.1 Analysis conditions

The simplified analysis condition based on an actual tunneling site was assumed to examine the performance of the proposed method in case of soft ground. The analysis length is approximately 67 m including a curve with a radius of 20 m from 21.4 m distance to 53.4 m distance. The overburden depth is approximately 24.1 m, and the groundwater level is GL-4.9 m, as shown in Figure 10. The ground properties are shown in Table 2. The ground reaction curves $K-U_n$ relationships for Ds and Dc layers are shown in Figure 11. This means that the tunnel is constructed around the boundary between the stiff soil Ds layer and the soft soil Dc layer. The dimensions of the shield and the tunnel are shown in Table 3, that is, the shield is an articulated shield type EPB shield with 2.0 m in outer radius and 6.655 m in total length.

3.2 Shield operation

3.2.1 Shield steering

The articulated shield with the dimensions in Table 3 was used in this study. Therefore,

$$\begin{aligned} L_{CSE} &= 2.490 \text{ m} \\ L_1 &= L_{M1} - L_{CSE} = 0.480 \text{ m} \\ L_2 &= L_{M2} - L_{CSE} = 1.195 \text{ m}, \end{aligned}$$

then the shield is categorized to type 2.

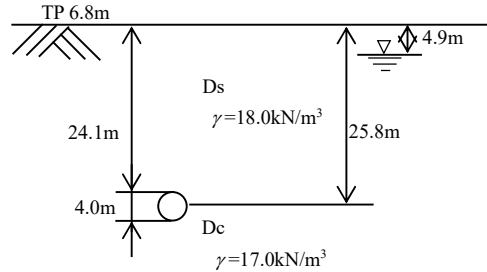


Figure 10 Geological profile

Table 2 Ground properties

Ground layer	Ds	Dc
Unit weight (kN/m ³)	18	17
Cohesion (kN/m ²)	0	206
Internal friction angle (deg)	36	0
$K_{ha} (= K_{hmin})$	0	0
K_{ho}	0.412	1
$K_{hp} (= K_{hmax})$	5	5
$K_{va} (= K_{vmin})$	0	0
K_{vo}	1	1
$K_{vp} (= K_{vmax})$	5	5
k_h (MN/m ³)	36.6	15.1
k_v (MN/m ³)	36.6	15.1
Coeff. of friction	0.1	0.1

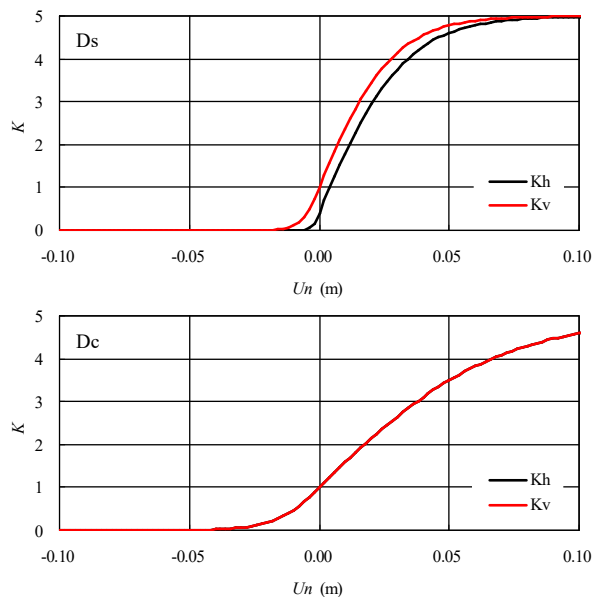


Figure 11 Ground reaction curve of the soils at the tunnel

Table 3 Dimensions of shield and tunnel

Item	Component	Value
Shield	Outer radius (m)	2.0
	Total length (m)	6.655
	Length of front body (m)	2.970
	Length of rear body (m)	3.685
	Length between crease center and segment front end (m)	2.490
	Self-weight (kN)	945
Shield jack	Number of jacks	16
	Radius of jack (m)	1.7
Segment	Outer radius (m)	1.95, 1.93
	Width (m)	1.2, 0.3
Tunnel	Horizontal curve radius (m)	20.00
	Slope (ascend)	0.6/1000
Ground	Ground water level (m)	GL-4.9
	Overburden depth (m)	24.1

The calculated articulation angles in horizontal and vertical directions are shown in Figure 12. The calculated distribution of overcut by the copy cutter on the excavated surface is shown in Figure 13. From these figures on shield steering, the following were found:

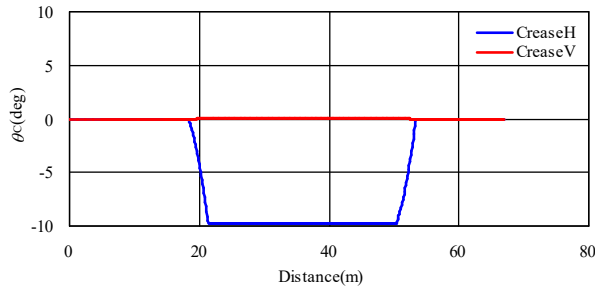


Figure 12 Articulated angle

- Around the beginning of the curve (BC)
 The articulation angle in horizontal direction, θ_{CH} , decreases from zero to -9.7 degrees around the BC. However, the articulation angle in vertical direction, θ_{CV} , is zero. The overcut by the copy cutter around the left spring line (90 degrees) is carried out from 19.8 m distance to 23.0 m distance, and around the right spring line (270 degrees), it starts from 21.4 m distance. The maximum copy cutter length, CCL , is 73 mm and 105 mm at the left spring line and the right spring line, respectively. These are because the shield starts to rotate to the rightward circular curve, and the rear end of the rear body needs the overcut at the convex side of the curve alignment around the BC. These come from the conditions 1 and 2 in “2.1.2. Calculation conditions.”
- Along the horizontal curve
 Along the horizontal curve alignment, the θ_{CH} , the θ_{CV} , and the overcut by the copy cutter are uniform. The θ_{CH} keeps a constant value, -9.7 degrees, the θ_{CV} is zero, and the CCL around the right spring line is always 92 mm. These are because the shield is in the horizontal circular curve, and the cutter face touches the trace of the front end of the rear body at the convex side of the curve, which needs the overcut at the concave side of the curve. These come from the conditions 3 and 4 in “2.1.2. Calculation conditions.”
- Around the end of the curve (EC)
 The θ_{CH} increases from -9.7 degrees to zero around the EC. However, the θ_{CV} is zero. The overcut by the copy cutter around the left spring line (90 degrees) is carried out from 54.4 m distance to 56.9 m distance, and around the right spring line (270 degrees), it ends at 55.1 m distance. The maximum copy cutter length, CCL , is 46 mm at the left spring line. These are

because the shield enters to the straight alignment, and the front end of the rear body needs the overcut at the convex side of the curve alignment around the EC. These come from the same reasons around the BC.

3.2.2 Shield operation data

The input data used for simulation are shown in Figure 14. The tunneling operations are jack thrust F_{3r} , horizontal jack moment M_{3p} (+: right turn), vertical jack moment M_{3q} (+: downward), cutter face (CF) rotation direction (1: counterclockwise direction, viewed from the shield tail), copy cutter length CCL , area of applied copy cutter CC range, and articulation angle in horizontal direction θ_{CH} (+: left turn), which are employed to control the shield position and the shield rotation during excavation. The shield rotation is defined as yawing angle ϕ_y (+:right turn) and pitching angle ϕ_p (+: downward). The excavation conditions are shield velocity v_s , slurry pressure σ_m , and slurry density γ_m in the chamber, which is usually controlled to stabilize the tunnel face.

F_{3r} is applied to the shield to drive the shield forward against earth pressure at the face and friction on the shield skin plate, as it advances. Since the planned tunnel alignments are horizontal rightward curves, M_{3p} is applied to negotiate the horizontal moment due to normal earth pressure around the skin plate M_{5p} . M_{3q} is mainly applied against the vertical moment due to the earth pressure on the cutter disc and the self-weight of the shield. Here, F_{3r} of approximately 7 MN was obtained by the sequential analysis using the kinematic shield model without jack force (F_{3r} , M_{3p} , and M_{3q} are zero). On the other hand, M_{3p} and M_{3q} were assumed to be zero as the initial values, since the sequential analysis, which does not consider the equilibrium conditions, provides eccentric values of M_{3p} and M_{3q} , especially at a sharp curve.

The sign of cutter torque defines the CF rotation direction, which generates the shear resistance on the cutter disc, and its rotation direction causes the shield rolling around its axis. Therefore, the rotation direction of the cutter disc is alternately controlled to maintain the use of facilities inside the shield. CCL and CC range were set, based on the required overcut shown in Figure 13, so that the shield is inside of the excavated area.

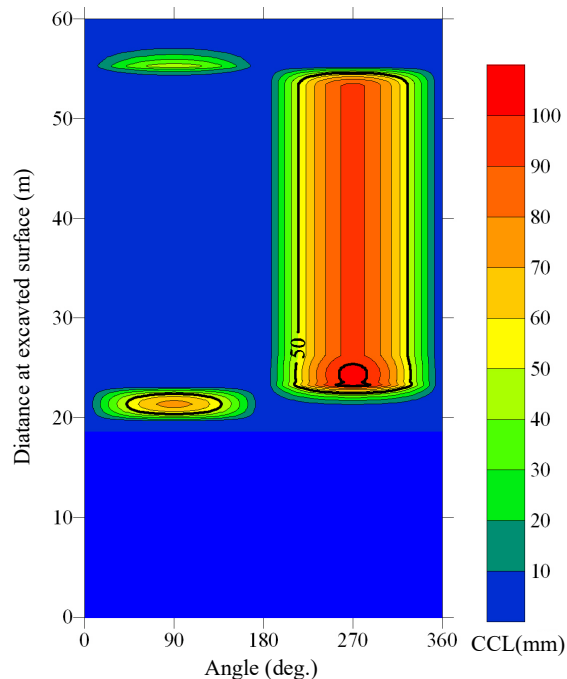


Figure 13 Distribution of overcut by copy cutter
 The copy cutter is used to increase the excavated area around the

cutter disc, which reduces the ground reaction force acting on the skin plate and makes a shield easily translate or rotate to this field. θ_{CH} corresponds to the horizontal curve radius of the tunnel alignment. The use of articulation of shield is to fit the skin plate to the area excavated by the cutter disk and copy cutter, which also reduces the ground reaction force acting on the skin plate and makes a shield easily translate or rotate.

ϕ_y shows that the rotation of the front body to follow the planned horizontal tunnel alignment at the rightward curve. ϕ_p is close to zero because the shield is on an almost horizontal plane.

Shield velocity v_s of 0.020 m/min and muck density γ_m of 15.0 kN/m³ were set, based on the experience. To stabilize the face, chamber pressure σ_m approximately 212 kPa is applied based on the lateral earth pressure at the tunnel face.

3.3 Shield behavior

3.3.1 Simulation using the original steering data

The shield behavior was simulated from 5.0 m distance to 66.9 m distance, based on the shield operational data in Figure 14. The shield operational data except for the shield steering data were modified so that the calculated shield behavior has a good agreement with the planned one.

Figure 15 shows the planned alignment and the calculated traces of the shield on vertical and horizontal planes. The calculated and planned time-dependent parameters ϕ_y , ϕ_p , and v_s are shown in Figure 16. From Figure 15, the following were found: 1) the shield moves upward gradually as the shield advances and the shield deviates approximately 0.5 m from the planned alignment at the end of the simulation; and 2) the shield direction on the horizontal plane can rotate approximately 90 degrees, but the shield cannot follow the planned horizontal alignment with a radius of 20 m. From Figure 16, the following were found: 1) the change rate of ϕ_y against the distance is smaller than the planned one, which corresponds to the tendency of the shield trace on the horizontal plane; 2) the ϕ_p is close to the planned ϕ_p , but the ϕ_p shows the lookup approximately 27 min at the end of the simulation; and 3) the v_s is close to the planned v_s , but the v_s increases at the end of the simulation up to approximately 0.035 m/min. These are considered as follows: 1) the overcut by the copy cutter and the articulation angle, which are obtained from the geometric conditions in “2.1.Shield steering,” are not enough to rotate the shield along a sharp curve with a radius of 20 m, since the difference of the ground reaction force between the left and right sides of the shield is smaller in the case of the soft soil; and 2) the ϕ_p looks up, then the shield moves upward, and the v_s increases due to the decrease of the face resistance.

3.3.2 Simulation using the modified steering data

From the above, the shield steering data were adjusted so that the calculated shield behavior has a good agreement with the planned one. Here, the calculated results are shown, when the copy cutter length, CCL , and the articulation angle in horizontal direction, θ_{CH} , become 1.2 times.

Figure 17 shows the planned alignment and the calculated traces of the shield on vertical and horizontal planes. The calculated and planned time-dependent parameters ϕ_y , ϕ_p , and v_s are shown in Figure 18. From Figure 17, the following were found: 1) the shield trace on vertical and horizontal planes have a good agreement with the planned one; and 2) the deviation in vertical plane is less than 0.1 m, and the deviation in horizontal plane is around 1 m. From Figure 18, the following were found: 1) the ϕ_y of the front body and

the v_s have a good agreement with the planned one; and 2) the ϕ_p is close to the planned one, but the ϕ_p decreases up to approximately 24 min at the end of the simulation.

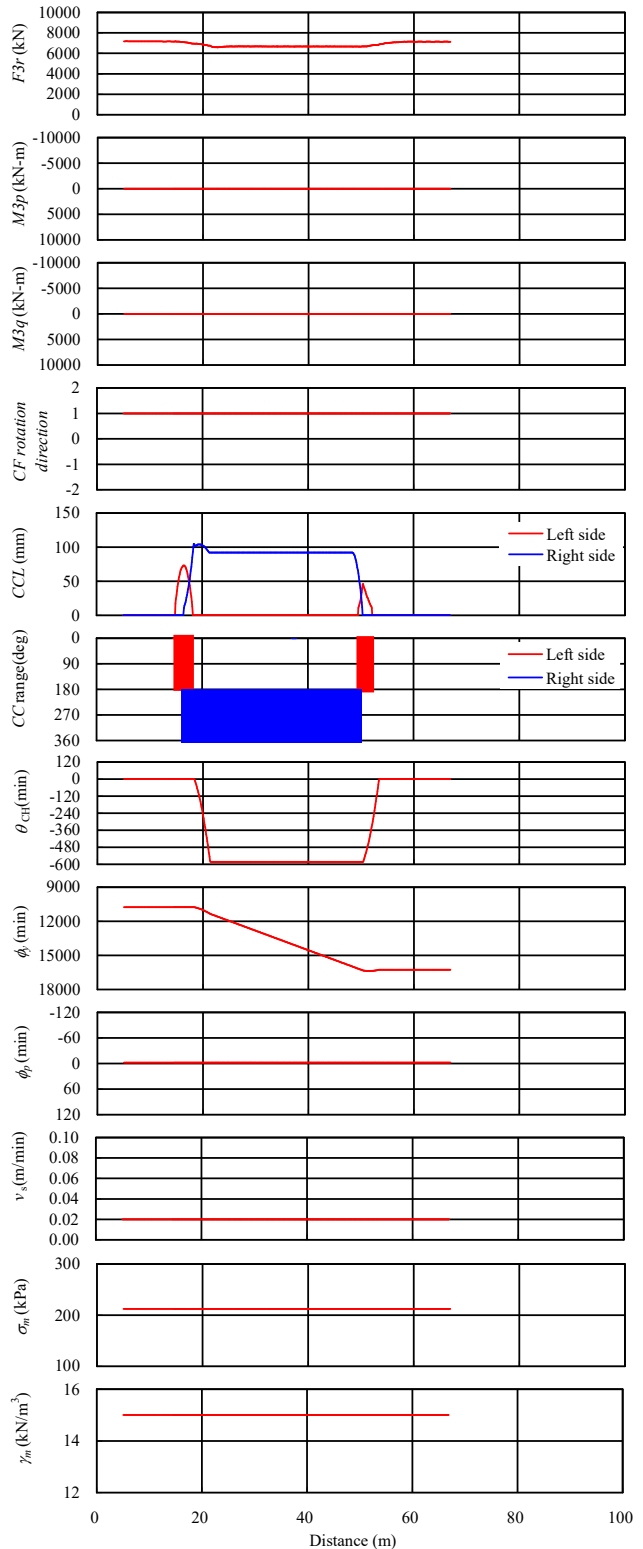


Figure 14 Shield operation data

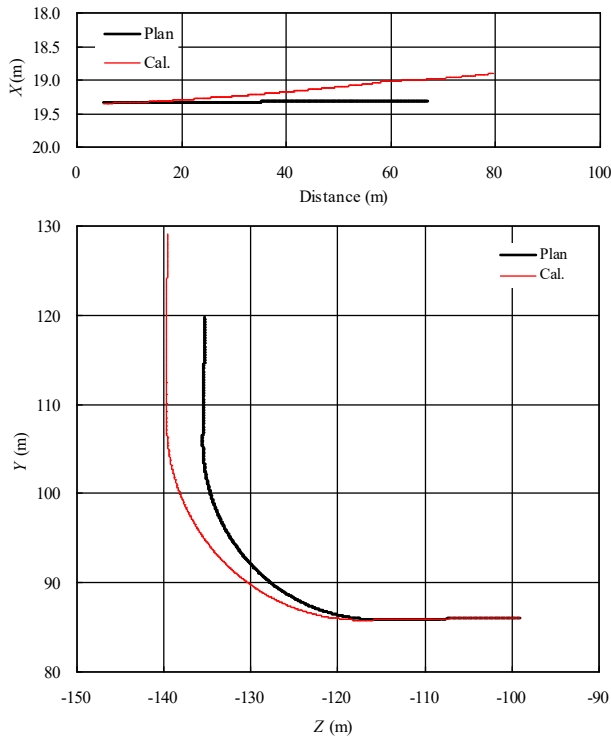


Figure 15 Calculated and planned shield traces (before correction)

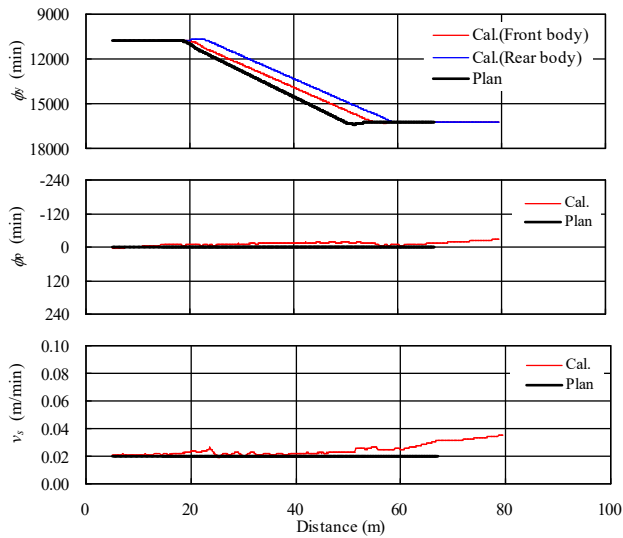


Figure 16 Calculated and planned shield behavior (before correction)

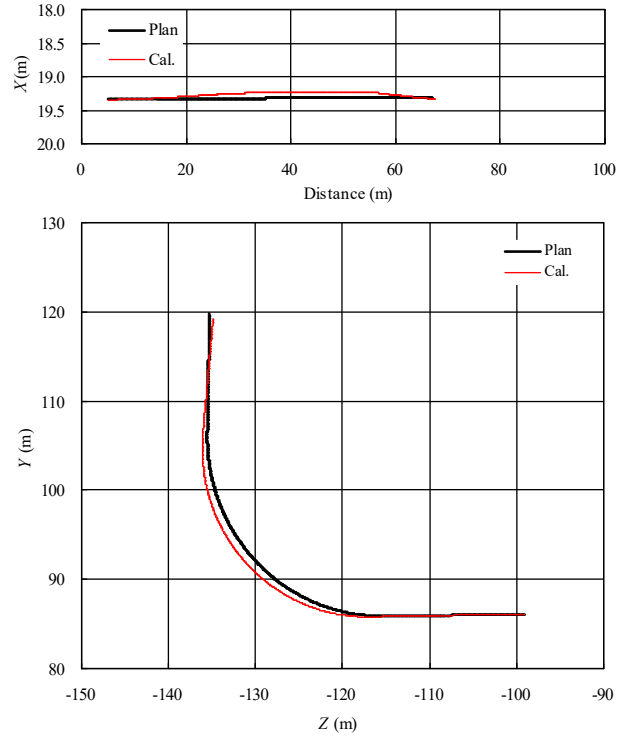


Figure 17 Calculated and planned shield traces (after correction)

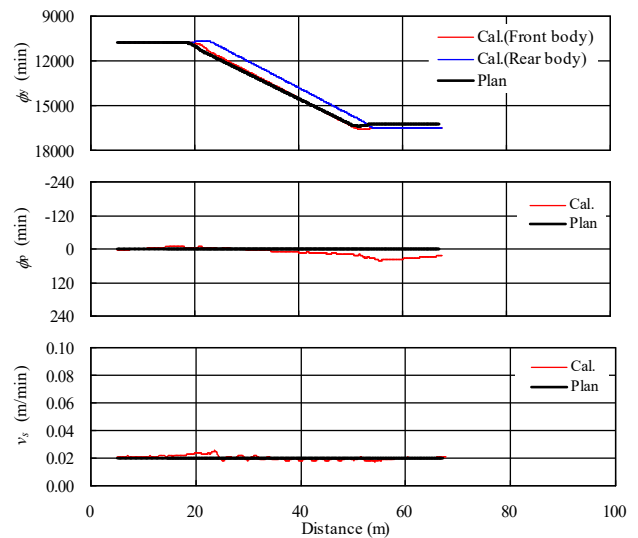


Figure 18 Calculated and planned shield behavior (after correction)

The following are then considered:

- 1) the revised copy cutter length and the articulation angle are proper, since these figures show overall good agreement between the calculated shield behavior and the planned one;
- 2) in practice, these differences can be adjustable by updating the shield operation on time, based on real-time measurement on shield position, rotation, etc.; and
- 3) when the copy cutter length and the articulation angle, which are determined based on the geometric conditions in “2.1. Shield steering,” are applied to the shield operation, it is necessary to consider the ground properties, especially in the case of soft soil.

4. CONCLUSIONS

The simulation of the articulated shield behavior at a straight line and curved alignment in soft ground was carried out using the shield operation data, as shown in Figure 14, and the kinematic shield model to examine the applicability of the proposed method for soft ground. The applicability of the calculated steering conditions for soft ground was discussed quantitatively, comparing the calculated shield behavior with the planned tunnel alignment. As a result, the following can be concluded:

1. The calculated steering conditions, that is, the copy cutter length and range, and the articulation angle and direction, are reasonable from the viewpoint of theory and site experience.
2. When the shield steering conditions, which are calculated from the geometric conditions in "2.1. Shield steering," are applied to the shield operation, the ground properties should be considered in case of soft soil.
3. When the proper shield operation data including the shield steering conditions are in use, the calculated shield behavior has a good agreement with the planned tunnel alignment.
4. The ground displacement, which is defined by the area excavated by copy cutter and the articulation of the shield, is a predominant factor affecting shield behavior, since it defines the ground reaction force acting on the shield. These facts also coincide with the practical experience.

5. REFERENCES

- Akagi, H., and Komiya, K. (1993) "Finite element analysis of the stress-deformation behavior of soil considering the execution procedures during shield work," *J. Japan Soc. Civ. Eng.*, 481(III-25), 59–68 (in Japanese).
- Alsahly, A., Stascheit, J., and Meschke, G. (2013) "Computational framework for 3D adaptive simulation of excavation and advancement processes in mechanized tunnelling," *Computational Methods in Tunnelling, EURO:TUN 2013 Ruhr University Bochum*, 85–96.
- Chaipayut, S., Huynh, T. N., and Sugimoto, M. (2015) "Influence of copy cutter length on H&V shield behavior," 15th Asian Regional Conference on Soil Mechanics and Geotechnical Engineering (15ARC), Fukuoka, Japan, ISSMGE.
- Chen, J. (2008) Study on calculation method of overcutting space and articulation angle during curved excavation by articulated shield, PhD thesis, Nagaoka Univ. of Technology, Niigata, Japan.
- Chen, J., Matsumoto, A., and Sugimoto, M. (2008) "Simulation of articulated shield behavior at sharp curve by kinematic shield model," *Geotechnical Aspects of Underground Construction in Soft Ground*, Balkema, Leiden, The Netherlands, 761–767.
- Clough, G. W., Sweeney, B. P., and Finno, R. J. (1983) "Measured soil response to EPB shield tunneling," *J. Geotech. Eng.*, 109(2), 131–149.
- Date, K., Igarashi, H., Sasakura T., and Yakeyama K. (1999) "A study of posture change prediction of multi-shield tunneling machine," *J. Japan Soc. Civil Eng.*, 630/VI-44, pp. 39–53 (in Japanese).
- Festa, D., Broere, W., and Bosch, J. W. (2013) "On the effects of the TBM-shield body articulation on tunnelling in soft soil," *Computational Methods in Tunnelling, EURO:TUN 2013 Ruhr University Bochum*, 109–118.
- Finno, R. J., and Clough, G. W. (1985) "Evaluation of soil response to EPB shield tunneling," *J. Geotech. Eng.*, 111(22), 155–173.
- Fujita, K. (1989) "Underground construction, tunnel, underground transportation: Special lecture B," *Proc. 12th Int. Conf. on Soil Mech. Found. Eng.*, Rio de Janeiro, Vol. 5, 2159–2176.
- Hansmire, W. H., and Cording, E. J. (1985) "Soil tunnel test section: Case history summary," *J. Geotech. Eng.*, 111(11), 1301–1320.
- Huynh, T. N., Chen, J., and Sugimoto, M. (2015) "Analysis on shield operational parameters to steer articulated shield," 15th Asian Regional Conference on Soil Mechanics and Geotechnical Engineering (15ARC), Fukuoka, Japan, ISSMGE.
- Huynh, T. N., Pham, V., Sugimoto, M., Tanaka, Y., Ohta, H., and Yasui, K. (2017) "Simulation of H&V shield behavior at sharp curve by kinematic shield model," *Geotechnical Engineering (Journal of SEAGS & AGSSEA)*, 48(2), in print.
- Kasper, T., and Meschke, G. (2004) "A 3D finite element simulation model for TBM tunneling in soft ground," *International Journal for Numerical and Analytical Methods in Geomechanics*, 28(14), 1441–1460.
- Komiya, K., Soga, K., Akagi, H., Hagiwara, T., and Bolton, M. D. (1999) "Finite element modelling of excavation and advancement processes of a shield tunneling machine," *Soils Found.*, 39(3), 37–52.
- Kuwahara, H., Harada, M., Seno, Y., and Takeuchi, M. (1988) "Application of fuzzy reasoning to the control of shield tunnelling," *Proc. Japan Soc. Civil Eng.*, 391/VI-8, 169–178 (in Japanese).
- Lee, K. M., Rowe, R. K., and Lo, K. Y. (1992) "Subsidence owing to tunneling: I. Estimating the gap parameter," *Can. Geotech. J.*, 29, 941–954.
- Lee, K. M., Ji, H. W., Shen, C. K., Liu, J. H., and Bai, T. H. (1999) "Ground response to the construction of Shanghai metro tunnel-line 2," *Soils Found.*, 39(3), 113–134.
- Matsumoto, A., Chen, J., and Sugimoto, M. (2009) "Simulation of articulated shield behavior along a sharply curved alignment in a multilayered ground," *Computational Methods in Tunnelling, EURO:TUN 2009, Ruhr University Bochum*, 83–90.
- Melis, M. J., and Medina, L. E. (2005) "Discrete numerical model for analysis of earth pressure balance tunnel excavation," *Journal of Geotechnical and Geoenvironmental Engineering*, 131(10), 1234–1242.
- Miki, A., Nagura, H., Kayukawa, K., Shimbara, K., Ehara, A., and Sugimoto, M. (2016) "Development of underground enlargement method using multiple shield tunnels at great depth and high water presser," *Proc. of Tunnel Engineering, JSCE*, 26, 1–12 (in Japanese).
- Muto, M., Ito, T., Usui, H., and Ishido, A. (2015) "Drive shield TBM longitudinally under a small river using the H&V shield spiral technique," *Tunnel and Underground Space, Japan Tunnelling Association*, 46(2), 17–23 (in Japanese).
- Rowe, R. K., Lo, K. Y., and Kack, G. J. (1983) "A method of estimating surface settlement above shallow tunnels constructed in soft ground," *Can Geotech. J.*, 20, 11–22.
- Rowe, R. K., and Lee, K. M. (1992) "Subsidence owing to tunneling: II Evaluation of prediction technique," *Can. Geotech. J.*, 29, 941–954.
- Sakai, K., and Hoshitani, M. (1987) "Prediction and control of behaviors on driving shields using Kalman filter theory," *Proc., Japan Soc. Civil Eng.*, 385/VI-7, 69–78 (in Japanese).
- Shield Tunnelling Association in Japan. (2011a) Leaflet on horizontal and vertical variation shield method, STA, Tokyo, Japan.
- Shield Tunnelling Association in Japan. (2011b) Leaflet on DPLEX shield method, STA, Tokyo, Japan.
- Shimizu, Y., and Suzuki, M. (1992a) "Study of the moving characteristics of shield tunneling machines," *J. Japan Soc. Mech. Eng.*, 58(550), 155–161 (in Japanese).
- Shimizu, Y., Furukawa, K., Imai, K., and Suzuki, M. (1992b) "Study of the moving characteristics of shield tunneling machines (2nd Report)," *J. Japan Soc. Mech. Eng.*, 58(554), 121–128 (in Japanese).
- Sramoon, A., and Sugimoto, M. (1999) "Development of a ground reaction curve for shield tunnelling," *Proc., Int. Symp. on Geotechnical Aspects of Underground Construction in Soft Ground*, Balkema, Rotterdam, The Netherlands, 437–442.
- Sramoon, A., Sugimoto, M., and Kayukawa, K. (2002) "Theoretical model of shield behavior during excavation II: Application," *Journal of Geotechnical and Geoenvironmental Engineering*, 128(2), 156–165.
- Sugimoto, M. (1995) "Modeling of acting load on shield," *Underground Construction in Soft Ground*, Balkema, Leiden, The Netherlands, 273–278.

- Sugimoto, M., and Sramoon, A. (2002a) "Theoretical model of shield behavior during excavation I: Theory," *Journal of Geotechnical and Geoenvironmental Engineering*, 128(2): 138–155.
- Sugimoto, M., Sramoon, A., Shimizu, T., Dan, A., and Kobayashi, T. (2002b) "Simulation of articulated shield behavior by in-situ data based on kinematic shield model," *Journal of Tunnel Engineering* 12: 471–476 (in Japanese).
- Sugimoto, M., Sramoon, A., Yamaguchi, T., and Miki, A. (2003) "Simulation on DPLEX shield behavior due to cutter frame rotation by kinematic shield model," *Journal of Tunnel Engineering* 13, 61–66 (in Japanese).
- Sugimoto, M., Sramoon, A., Konishi, S., and Sato, Y. (2007) "Simulation of shield tunnelling behavior along a curved alignment in a multilayered ground," *Journal of Geotechnical and Geoenvironmental Engineering*, 133(6): 684–694.
- Szechy, K. (1966) *The art of tunneling*, Akademiai Kiado, Budapest.
- Takeda, H., Kusabuka, M., Yoshida, T., Tanaka, H., and Kurokawa, N. (1998) "Finite element analysis of general contact problems application for excavation of shield tunnel," *J. Japan Soc. Civil Eng.*, 603/III-44, pp. 1–10 (in Japanese).